PHYSICAL REVIEW B VOLUME 26, NUMBER 7 1 OCTOBER 1982

Jahn-Teller stress effects on the magnetization and ESR properties of LaSb:Dy single crystals

J. M. Bloch* and D. Davidov
Racah Institute of Physics, The Hebrew University of Jerusalem, Israel
(Received 5 November 1981)

We demonstrate that the ion-lattice interaction plays a significant role in the magnetization and ESR properties of LaSb:Dy single crystals. We provide a free-energy calculation to demonstrate that the applied magnetic field distorts locally the crystal around the Dy ion leading to a deviation of the Dy magnetic moment with respect to that expected from "pure" crystal-field effects. The fitting of the experimental magnetization data, measured along the [001] direction, to the theory based on our free-energy calculation, enables us to extract the coupling constant between the Γ_3 strain modes and the Dy ion to be $|V(\Gamma_3)| = 24$ K. Analysis of the angular dependence of the ESR line shape strongly supports the hypothesis that only Γ_3 strains play a role in the ESR experiment. The combined ESR and magnetization data yield the width of the Γ_3 strain distribution to be $\sigma_3 = 1.25 \times 10^{-3}$. Using the value $V(\Gamma_3) = 24$ K, our free-energy calculation clearly shows softening of the elastic constants of force at low temperatures. This can provide a mechanism for the large strain effects in our ESR. It indicates "single-ion" Jahn-Teller effects in LaSb:Dy at low temperatures.

I. INTRODUCTION

The existence of Jahn-Teller effect in rare-earth intermetallic compounds and alloys was pointed out only in the last decade.[1,2] In these rare-earth compounds mainly collective Jahn-Teller effects have been observed which are manifested by a phase transition involving symmetry-lowering distortion and magnetic transition. There are very few reports on Jahn-Teller for rare-earth dilute alloys except the work of Dixon on Pd:ER (Ref. 3) (and even here the situation is not so clear[3]). Among the rare-earth compounds undergoing a "cooperative Jahn-Teller" transition one should mention the metallic cubic compound DySb which exhibits simultaneous antiferromagnetic ordering and structural transition (from cubic to a tetragonal phase) at $T_c = 9.5$ K (Refs. 4–8). This transition was interpreted by the existence of three types of interactions having equal magnitude, namely, the Jahn-Teller distortive interaction, the bilinear exchange interaction, and the biquadrupole interaction.[4–6]

This paper reports magnetization study and ESR measurements on $Dy_xLa_{1-x}Sb$ single crystals in the dilute limit. In this limit the biquadratic and bilinear exchange interactions are negligible and the dominant interaction is the Jahn-Teller interaction between the Dy ions and the lattice modes. We shall demonstrate that both ESR and magnetization measurements provide strong evidence for the existence of "single-ion" Jahn-Teller effects at low temperatures.

II. EXPERIMENTAL RESULTS

The magnetization of LaSb:Dy single crystals for at least five samples with nominal Dy concentrations between 0.5 and 6 at.% were measured at low temperatures using a vibrating-type magnetometer. The insert of Fig. 1 yields a typical angular dependence of the magnetization for our 0.9% sample at $T = 4.1$ K and $H = 17$ kG. The angle θ in this insert is the angle between the magnetic field and the [001] direction in the (011) plane of rotation. The dependence of the magnetization on the external field along the [001] direction is shown in Fig. 1. On the same figure we have shown an attempt to fit the angular dependence and the field dependence of the magnetization to a crystalline-field–only Hamiltonian [see Eq. (2) below] and the crystalline-field parameters $x = -0.84$, $W = 0.4$ K (in the notations of Lea, Leask, and Wolf[9]) taken from the paper of Bucher *et al.*[4] As clearly seen, the magnetization cannot be explained by such crystalline-field–Hamiltonian and such parameters. We have tried to find other parameters including those of Kouvel[10] to fit the experimental data (and especially the ratio $\mu[100]/\mu[111]$) but the agreement is bad. In this fitting procedure we have calculated the Dy concentration by fitting the slope of the low-field magnetization to the theory. The calculated concentrations do not differ from the nominal Dy concentration by more than 5%.

The ESR measurements were conducted mainly at

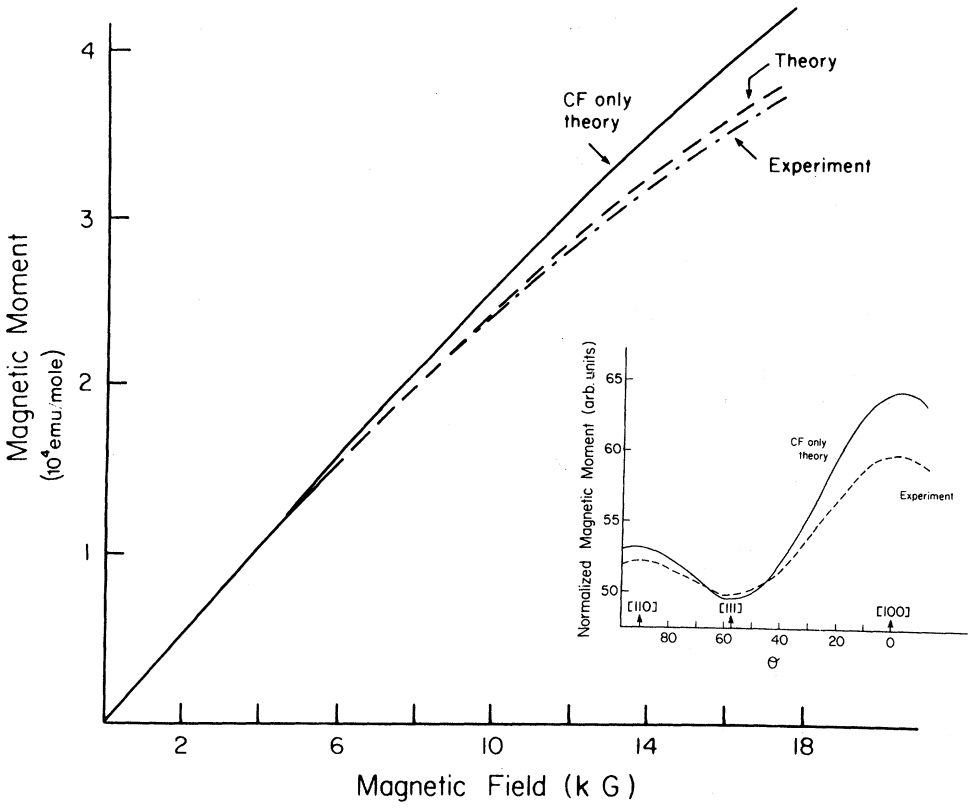

FIG. 1. Magnetization as a function of field for magnetic field along the [001] direction of LaSb:Dy (0.9 at.%) single crystal at $T=4.1$ K. The solid line is a fit to a crystalline-field–only Hamiltonian. The dashed line is a theoretical fit using the procedure described in text with the parameters $x=-0.84$, $W=0.4$ K, $C(\Gamma_3)=420.000$ K/ion, $|V(\Gamma_3)|=24$ K, $H=17$ kG, $-0.02\leq\epsilon(\Gamma_{3g\theta})$; $\epsilon(\Gamma_{3g\epsilon})\leq 0.02$. Insert: The angular dependence of the magnetic moment of LaSb:Dy (1 at.%) single crystal rotated in the (011) plane. The dashed line represents the experimental data. The solid line is a theoretical curve using the crystalline-field Hamiltonian [Eq. (2)] only with the parameters $x=-0.84$, $W=0.4$ K.

X-band frequency with only few measurements at Q band. The temperature was varied from 2 to 22 K. The ESR spectra exhibit a strong anisotropy as a function of the orientation of the magnetic field. Figure 2 exhibits the angular dependence of the ESR line shape of one of our LaSb:Dy samples at $T=4.1$ K (the same sample on which magnetization was measured). The sample was rotated in the (011) plane and θ measures the angle between the magnetic field and the [001] direction in the plane of rotation. As clearly seen, the ESR line exhibits a minimum linewidth with a Dysonian line shape for an angle $\theta\simeq 55°$ approximately, i.e., for magnetic field in the [111] direction. For this particular angle the field for resonance corresponds to a g value of $g=6.60\pm 0.1$, appropriate to a Γ_6 crystal-field ground state. For other directions the linewidth significantly increases as one goes from the [111] direction towards the [001] direction or the [110] direction. In the [001] and [110] directions the linewidth is so large that any line-shape analysis is meaningless. Away from the [111] direction the ESR line shape is not regular and exhibits in many cases what appears to be a "structure" on the line (see Fig. 2).

Practically, the same general behavior was observed for at least 15 different samples with different Dy concentrations (in the range 5000 ppm to 6 at.%) grown under slightly different conditions and heat treatment. However, we did observe slight differences in the angular dependence of the ESR line shape which indicate that this angular dependence is also sample dependent to some extent. There is no clear correlation between the observed angular dependence and the Dy concentration or heat treatment.

The results at higher temperatures (i.e., $T=7$, 15, 22 K) exhibit a similar angular dependence of the ESR line shape without any significant broadening or narrowing of the ESR lines, but there is a drop in the line intensity as the temperature is increased. The ESR results of the Q band ($T=4.1$ K) show very similar angular dependence with faster increase of the

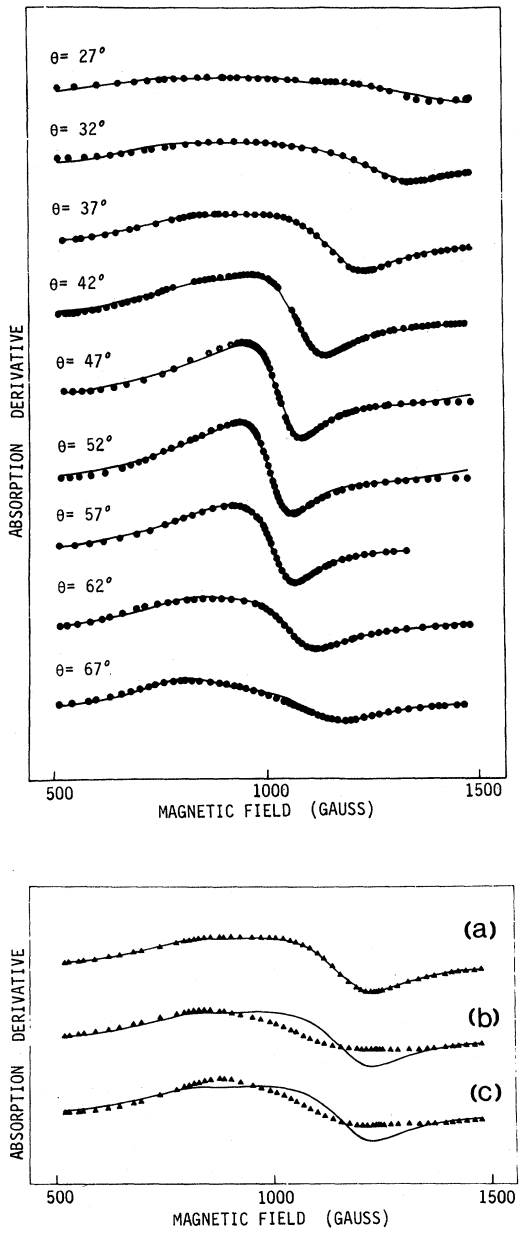

FIG. 2. Upper part: ESR spectra (solid lines) of LaSb:Dy (2000 ppm) at 4.1 K, X band, and for several orientations of the magnetic field. θ measures the angle between the magnetic field and the [001] direction in the (110) plane. The circles represent theoretical fits using the procedure described in the text and the parameters $g=6.60\pm0.1$, $D=70$ G and $|g_3\sigma_3|=1.6\pm0.3$; $|g_5\sigma_5|=0$. Lower part: ESR spectra (solid line) for LaSb:Dy (2000 ppm) at $T=4.1$, $\theta=37°$. The triangle represents theoretical fits using the procedure described in the text. In (a) the parameters are $|g_3\sigma_3|=1.6$, $|g_5\sigma_5|=0$; (b) $|g_3\sigma_3|=0$, $|g_5\sigma_5|=1.32$; and (c) $|g_3\sigma_3|=1.6$ and $|g_5\sigma_5|=1.32$. As clearly seen the presence of Γ_5 strain modes leads to a large deviation from the experimental spectra.

linewidth as one rotates the magnetic field from the [111] direction towards the [001] and [011] directions, much faster with respect to the results at X band.

The crystalline-field parameters of Bucher *et al.*[4] predict Γ_6 ground state with Γ_8 (Ref. 4) first excited state at 14.5 K. The crystalline-field level splitting given by Kouvel *et al.*[10] for DySb is slightly different. For Γ_6 ground state, one expects isotropic ESR line, i.e., a completely different behavior from our results in Fig. 2. It should be mentioned that preliminary ESR data on LaSb:Dy were reported previously and were interpreted by a random stress model using second-moment calculations.[11,12] Clearly the "structure" on the ESR lines (Fig. 2) does not allow such an approximation to interpret our data.

III. ANALYSIS

We believe that both the magnetization and ESR results can be explained by a coupling term between the Dy ion and lattice modes. We consider a cluster composed of Dy ion and its six nearest-neighbor Sb ions (Fig. 3). There are 21 degrees of freedom associated with the seven ions in the cluster[13] of which six must be subtracted out as being pure translation or rotation. The remaining 15 can be grouped into six even strain modes (or deformations) and nine odd strain modes. Neglecting the odd strain modes which might be important in the presence of a large magnetic field,[14] the six even deformations are divided into three groups of strain modes, namely, a Γ_{1g},

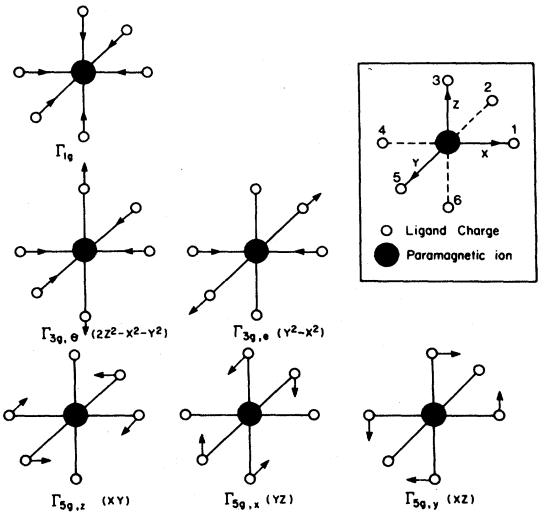

FIG. 3. Normal modes (even) for a cluster composed of the Dy ion and its six Sb nearest neighbors in NaCl structure. The insert yields the coordinate system.

two Γ_{3g}, and three Γ_{5g}. These strain modes are shown in Fig. 3. The total Hamiltonian $\mathcal{H}$ of "single ion" can be expressed, therefore, as the sum of the ionic Hamiltonian, $\mathcal{H}_I$, the lattice Hamiltonian, $\mathcal{H}_L$, and the lattice-ion coupling term $\mathcal{H}_{I-L}$. We write for the total Hamiltonian

$$\mathcal{H}=\mathcal{H}_I+\mathcal{H}_L+\mathcal{H}_{I-L} \ , \tag{1}$$

where

$$\mathcal{H}_I=g_J\mu_B\vec{H}\cdot\vec{J}+W\left[x\frac{O_4}{F(4)}+(1-|x|)\frac{O_6}{F(6)}\right] \ . \tag{2}$$

The first term is the Zeeman interaction and the second term is the crystalline-field Hamiltonian defined by Lea, Leask, and Wolf.[9] The lattice Hamiltonian is given by

$$\mathcal{H}_L=\tfrac{1}{2}C(\Gamma_1)\epsilon^2(\Gamma_1)+\tfrac{1}{2}C(\Gamma_3)[\epsilon^2(\Gamma_{3g\theta})+\epsilon^2(\Gamma_{3ge})]+\tfrac{1}{2}C(\Gamma_5)[\epsilon^2(\Gamma_{5gx})+\epsilon^2(\Gamma_{5gy})+\epsilon^2(\Gamma_{5gz})] \ , \tag{3}$$

where the deformations (strain modes) ϵ and the elastic constants of force, C, are defined by

$$\begin{aligned}
&\epsilon(\Gamma_{1g})=\epsilon_{xx}+\epsilon_{yy}+\epsilon_{zz}, \quad C(\Gamma_1)=\tfrac{1}{3}(C_{11}+2C_{12}),\\
&\epsilon(\Gamma_{3g\theta})=2\epsilon_{zz}-\epsilon_{xx}-\epsilon_{yy}, \quad C(\Gamma_3)=\tfrac{2}{3}(C_{11}-C_{12}),\\
&\epsilon(\Gamma_{3ge})=\epsilon_{xx}-\epsilon_{yy}, \quad C(\Gamma_5)=C_{44},\\
&\epsilon(\Gamma_{5gz})=\epsilon_{xy},\\
&\epsilon(\Gamma_{5gx})=\epsilon_{yz},\\
&\epsilon(\Gamma_{5gy})=\epsilon_{xz},
\end{aligned} \tag{4}$$

where ϵ_{ij} and C_{ij} are defined by Mullen *et al.*[5]: The constant of force as measured for DySb are given by Mullen *et al.*[5]

Finally the ion-lattice coupling Hamiltonian, $\mathcal{H}_{I-L}$ is given by

$$\mathcal{H}_{I-L}=V(\Gamma_3)[O(\Gamma_{3g\theta})\epsilon(\Gamma_{3g\theta})+O(\Gamma_{3ge})\epsilon(\Gamma_{3ge})]+V(\Gamma_5)[O(\Gamma_{5gz})\epsilon(\Gamma_{5gz})+O(\Gamma_{5gx})\epsilon(\Gamma_{5gx})+O(\Gamma_{5gy})\epsilon(\Gamma_{5gy})] \ , \tag{5}$$

with

$$\begin{aligned}
&O(\Gamma_{3ge})=3J_z^2-J(J+1) \ ,\\
&O(\Gamma_{3ge})=\sqrt{3}(J_y^2-J_x^2) \ ,\\
&O(\Gamma_{5gz})=\tfrac{1}{2}(J_yJ_x+J_xJ_y) \ ,\\
&O(\Gamma_{5gx})=\tfrac{1}{2}(J_zJ_y+J_yJ_x) \ ,\\
&O(\Gamma_{5gy})=\tfrac{1}{2}(J_zJ_x+J_xJ_z) \ .
\end{aligned} \tag{6}$$

$V(\Gamma_i)$ are the magnetoelastic coupling constants.

We shall analyze the magnetization along the [100] direction. In this analysis we shall neglect the Γ_5 type of distortions. It should be noted that the tetragonal distortion in DySb indicates the dominance of Γ_{3g} type of modes. Furthermore, we shall adapt the crystalline-field parameters of Bucher[4] $x=-0.84$, $W=0.4$ K and the elastic and magnetoelastic coupling constants $V(\Gamma_3)=24$ K and $C(\Gamma_3)=420.000$ K/ion from Mullen *et al.*[5] This enables one to calculate the eigenvalues of Eq. (1) by complete diagonalization of the 16×16 matrix appropriate to $J=\frac{15}{2}$ of Dy^{3+}. The eigenvalues observed in this way depend on $\epsilon(\Gamma_{3g\theta})$ and $\epsilon(\Gamma_{3ge})$ and the given magnetic field and temperature. This enables us to calculate the free energy defined by

$$F=k_BT\ln\sum_i\exp(-E_i/k_BT) \ , \tag{7}$$

where $\{E_i\}$ are eigenvalues of (1). The free energy calculated in this way is a function of $\epsilon(\Gamma_{3g\theta})$ and $\epsilon(\Gamma_{3ge})$. The free energy (surface) as a function of $\epsilon(\Gamma_{3g\theta})$ and $\epsilon(\Gamma_{3ge})$ is given as an example in Fig. 4 for different directions of the magnetic field. In all cases, $H=17$ kG, $T=4.2$ K were used, i.e., the same condition under which the angular dependence of the magnetization was measured. The most striking feature of Fig. 4 is the existence of minima in the free-energy surface which strongly depend on the magnetic field orientation. Particularly for $\vec{H}$ along the [001] direction a single minima is clearly seen [Fig 4(a)]; for $\vec{H}$ along the [111] direction three minima are observed since the three cubic principal axes are equivalent; for $\vec{H}$ along the [011] direction two minima are seen. The minima in the free energy F correspond to the most probable distortion which the Dy ions would experience. At high temperatures and in the absence of a magnetic field, the F surface maintains a symmetric form around $\epsilon(\Gamma_{3g\theta})=\epsilon(\Gamma_{3ge})=0$, which is consistent with the cubic symmetry (but see discussion below).

We argue that the free-energy calculation can ex-

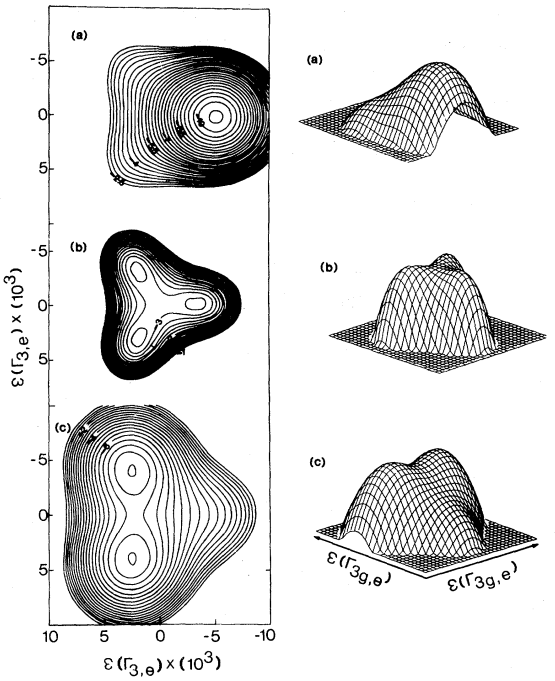

FIG. 4. Right side: The free energy, F, as a function of the strains $\epsilon(\Gamma_{3g\theta})$ and $\epsilon(\Gamma_{3ge})$. The free-energy surface (reversed) was calculated using the parameters $x=-0.84$, $W=0.4$ K, $V(\Gamma_3)=24$ K, $C(\Gamma_3)=420.000$ K/ion, and $H=17$ kG. In (a) the magnetic field is along the [001] direction, in (b) the magnetic field is along the [111] direction, and in (c) the magnetic field is along the [011] direction. Left side: The projection of the free-energy surface, F on the $\epsilon(\Gamma_{3g\theta})$ and $\epsilon(\Gamma_{3ge})$ plane. As clearly seen, the free energy exhibits in (a) a shallow minimum for $\vec{H}$ along the [001] direction, in (b) three minima for $\vec{H}$ along the [111] direction, and in (c) two minima for $\vec{H}$ along the [011] direction.

plain both the magnetization and the ESR data. The distortion produced by the magnetic field modifies the energy levels and consequently the magnetic moment. One can use the "most stable" distortion, with $\epsilon(\Gamma_{3g\theta})$ and $\epsilon(\Gamma_{3ge})$ represented by the minima in our free-energy surface (Fig. 4) in order to calculate the Dy^{3+} magnetic moment as follows:

$$\mu(\epsilon) \equiv \mu[\epsilon(\Gamma_{3g\theta}), \epsilon(\Gamma_{3ge})] = \frac{\sum \mu(E_i) \exp(-E_i/k_BT)}{\sum_i \exp(-E_i/k_BT)} . \quad (8)$$

Here $\mu(E_i)$ is the magnetic moment associated with the energy level E_i, and E_i are eigenvalues of (1). However, as can be clearly seen, the minima in the free energy are very shallow even in the presence of $H=17$ kG, which means that at $T=4.2$ K all that part of the free-energy surface in the vicinity of the minima has a finite probability to be populated. In short, the Dy ions are exposed to a large range of strains and a proper calculation of the magnetic moment, $\langle\mu\rangle$, requires averaging over the free-energy surface $F(\epsilon)$ as follows:

$$\mu = \frac{\sum \mu(\epsilon) \exp[-F(\epsilon)/k_BT]}{\sum \exp[-F(\epsilon)/k_BT]} , \quad (9)$$

where $\mu(\epsilon)$ is given by Eq. (8). The summation in (9) was carried over the following range of strains: $-0.02 \leq \epsilon(\Gamma_{3g\theta}) \leq 0.02$; $-0.02 \leq \epsilon(\Gamma_{3ge}) \leq +0.02$.

Figure 1 exhibits the fit of (9) to our magnetization along the [001] direction. We have used the parameters $x=-0.84$, $W=0.4$ K, $C(\Gamma_3)=420.000$ K/ion, and $|V(\Gamma_3)|=24$ K. The value $|V(\Gamma_3)|=24$ K is very close to that observed by Mullen *et al.* for DySb.[5]

We turn now to discuss our ESR results. Generally speaking, the ESR results can be analyzed by diagonalization of the Hamiltonian composed of $\mathcal{H}_I + \mathcal{H}_{I-L}$ in Eqs. (2) and (5). Such a diagonalization yields the energy levels $E(\Gamma_6, \pm\frac{1}{2})$ associated with the Γ_6 ground state as affected by the admixture with the Γ_8 excited state which is very sensitive to the presence of strains and external magnetic field. However, the ESR measurements were performed at relatively low temperatures such that only the first excited state, $\Gamma_8^{(1)}$, is populated. In such a case only six levels associated with the Γ_6 ground state and the $\Gamma_8^{(1)}$ first excited state are important. It is convenient, therefore, to work in the frame of the spin Hamiltonian suggested by us previously.[11] This will require a diagonalization of 2×2 matrix rather than 16×16 matrix. Furthermore, since most of the data on random stresses in metals[11,12] have been analyzed using a similar spin Hamiltonian, it has the advantage that one can compare the same parameters using a different set of experiments.

The spin Hamiltonian $\mathcal{H}_s$ is obtained by taking all possible multiplications of $\epsilon(\Gamma_i)$, H_j, and S_j ($j=x,y,z$) which are invariant under cubic operations. Following Ref. 11, we write

$$\mathcal{H}_s = g\mu_B\vec{H}\cdot\vec{S} + g_1\mu_B\vec{H}\cdot\vec{S}\epsilon(\Gamma_{1g}) + g_3\mu_B[(3H_zS_z - \vec{H}\cdot\vec{S})\epsilon(\Gamma_{3g\theta}) + \sqrt{3}(H_xS_x - H_yS_y)\epsilon(\Gamma_{3ge})] + g_5\mu_B[\tfrac{1}{2}(H_yS_z + H_zS_y)\epsilon(\Gamma_{5gx}) + \tfrac{1}{2}(H_zS_x + H_xS_z)\epsilon(\Gamma_{5gy}) + \tfrac{1}{2}(H_xS_y + H_yS_x)\epsilon(\Gamma_{5gz})] , \quad (10)$$

where $\vec{S}$ is the operator of angular momentum describing the doublet, g is the g value associated with the Γ_6 ground state, g_i ($i=1,3,5$) are constants which were calculated using a second-order perturbation theory in

$\mathcal{H}_{L-I}+\mathcal{H}_z$ [Eqs. (5) and (2), respectively] between the unperturbed energy levels of $\mathcal{H}_{cf}$. Such a calculation yields a relation between g_i and the magnetoelastic coupling constant $V(\Gamma_i)$ as follows

$$g_3=-2g_J V(\Gamma_3)\frac{\langle\Gamma_6\tfrac{1}{2}|3J_z^2-J(J+1)|\Gamma_8\tfrac{1}{2}\rangle\langle\Gamma_8\tfrac{1}{2}|J_z|\Gamma_6\tfrac{1}{2}\rangle}{E(\Gamma_8^{(1)})-E(\Gamma_6)}, \tag{11}$$

$$g_5=-4g_J V(\Gamma_5)\frac{\langle\Gamma_6\tfrac{1}{2}|J_xJ_z+J_zJ_x|\Gamma_8,-\tfrac{1}{2}\rangle\langle\Gamma_8-\tfrac{1}{2}|J_z|\Gamma_6-\tfrac{1}{2}\rangle}{E(\Gamma_8^{(1)})-E(\Gamma_6)},$$

where $|\Gamma_6 i\rangle$ and $|\Gamma_8^{(1)} i\rangle$ are unperturbed wave functions associated with the Γ_6 and the $\Gamma_8^{(1)}$ energy levels of the unperturbed Hamiltonian $\mathcal{H}_{cf}$.

The energy levels $\tilde{E}(\Gamma_6\pm\frac{1}{2})$ in the presence of strains and magnetic field can be calculated by diagonalization of the 2×2 matrix formed by the spin Hamiltonian. We find

$$\tilde{E}(\Gamma_6,\pm\tfrac{1}{2})=\pm\tfrac{1}{2}(\alpha^2+\beta^2+\gamma^2)^{1/2}, \tag{12}$$

which leads to energy splitting between the $\pm\frac{1}{2}$ levels of the Γ_6 ground state to be

$$\Delta\tilde{E}=(\alpha^2+\beta^2+\gamma^2)^{1/2}=H_r\cdot S(\vec{n}), \tag{13}$$

where H_r is the field for resonance and the angular dependence is given by $S(\vec{n})$ with $\vec{n}$ as a unit vector in the direction of $\vec{H}$: α, β, and γ are given as

$$\begin{aligned}\alpha&=g\mu_B H_x+g_3\mu_B H_x[-\epsilon(\Gamma_{3g\theta})+\sqrt{3}\epsilon(\Gamma_{3ge})]+g_5\mu_B[H_z\epsilon(\Gamma_{5gy})+H_y\epsilon(\Gamma_{5gz})],\\ \beta&=g\mu_B H_y+g_3\mu_B H_y[-\epsilon(\Gamma_{3g\theta})-\sqrt{3}\epsilon(\Gamma_{3ge})]+g_5\mu_B[H_x\epsilon(\Gamma_{5gz})+H_z\epsilon(\Gamma_{5gx})],\\ \gamma&=g\mu_B H_z+2g_3H_z\epsilon(\Gamma_{3g\theta})+g_5\mu_B[H_y\epsilon(\Gamma_{5gx})+H_x\epsilon(\Gamma_{5gy})].\end{aligned} \tag{14}$$

For particular set of distortions $\epsilon(\Gamma_{3g\theta})$, $\epsilon(\Gamma_{3ge})$, $\epsilon(\Gamma_{5gx})$, $\epsilon(\Gamma_{5gy})$, $\epsilon(\Gamma_{5gz})$, the field for resonance H_r is given by $H_r=h\nu/S(\vec{n})$, where $h\nu$ is the microwave energy and $S(\vec{n})$ is given by Eq. (13). We shall assume Gaussian distributions of strains given by

$$f[\epsilon(\Gamma_i)]=\frac{1}{(2\pi\sigma_i)^{1/2}}\exp\left(-\frac{\epsilon^2(\Gamma_i)}{2\sigma_i^2}\right). \tag{15}$$

Here σ_i $(i=3,5)$ are the width of the distribution associated with the Γ_3 strains and Γ_5, respectively. Note that the distribution of $\epsilon(\Gamma_{3g\theta})$ and $\epsilon(\Gamma_{3ge})$ should be identical as the cubic symmetry of lattice is preserved. Similarly, the distribution for the three strains $\epsilon(\Gamma_{5gx})$, $\epsilon(\Gamma_{5gy})$, and $\epsilon(\Gamma_{5gz})$ is the same. Consequently, the width of the distributions depends on two parameters only, namely, σ_3 and σ_5. Such distributions of strains similar to (15) creates distribution among the values of H_r. This last distribution will be denoted by $P(H_r)$ and is not necessarily a Gaussian but depends on σ_3 and σ_5. The ESR line shape will be given as a convolution of the distribution in H_r, $P(H_r)$, and the unperturbed ESR line shape. For the unperturbed ESR line shape we have chosen a Dysonian line shape (derivative) given by[15]

$$F(H)=\frac{\alpha(1-x^2)-2x}{(1+x^2)^2}, \tag{16}$$

where x is defined by $x=(H-H_r)/D$; D is the width at half maximum of the Dysonian line shape and α is a parameter determining the amount of dispersion and absorption in the total line shape $F(H)$. The unperturbed line shape (16) agrees well with the ESR line shape observed for the magnetic field in the [111] direction where the effect of strains can be neglected.

We expect the experimental line shape to be a convolution as follows:

$$L(H)=\int_{-\infty}^{+\infty}\frac{\alpha(1-x^2)^2+2x}{(1+x^2)^2}P\left(\frac{Dx}{H}\right)D\,dx. \tag{17}$$

Certainly all the information of the strains is incorporated in $P(H_r)$. Since $P(H_r)$ cannot be expressed explicitly, we have adapted a Monte Carlo method using a computer to calculate the integral in (17). The computer program to calculate (17) is given elsewhere.[16] The mathematical method can be described shortly as follows. We consider five groups of arbitrary numbers; each group is actually a Gaussian distribution of numbers. The five groups of numbers correspond to five distributions of strains (i.e., $\Gamma_{3g\theta}$, Γ_{3ge}, Γ_{5gx}, Γ_{5gy}, Γ_{5gz}) and consequently the width of the distributions are σ_3 for the first two groups and σ_5 for the last three groups of numbers. Each group contains 3500 numbers and the quality of the distribution was checked using well-known statistical methods. Each set of five numbers [corresponding to five values of $\epsilon(\Gamma_3)$ and $\epsilon(\Gamma_5)$] yield a value for $\Delta\tilde{E}$ [Eq. (14)] and consequently a value for H_r. In this way we have observed a group of values for H_r which yield the distribution $P(H_r)$. For each value H_r we have calculated x_i $(x_i=H-H_r^i/D)$. The values of x_i are substituted into a formula for the "theoretical line shape" given by

$$\tilde{L}(H)=\sum_{i=1}^{3500}\frac{\alpha(1-x_i^2)-2x_i}{(1+x_i^2)^2}. \tag{18}$$

The line shape observed using (18) was checked to

ensure statistical stability.

Figure 2 yields the experimental ESR line shape (solid lines) and the best fit of theory (circles) to the experiment. The fit was done by minimalization of the sum of the square of the deviations between the experimental points and the calculated points describing the line shape. In the fitting procedure, the following parameters have been taken into consideration: (a) the value of $D \simeq 70$ G, i.e., the width of the ESR line for $\vec{H}$ parallel to the [111] direction, (b) the width of the Gaussian distributions σ_3 and σ_5, (c) the values of g_3 and g_5, (d) the direction of the magnetic field with respect to the crystal axis, and (e) the resonance frequency.

The best fit of our theory to the ESR experimental line shape of LaSb:Dy (2000 ppm) yields

$$|g_3\sigma_3| = 1.6 \pm 0.3 \ , \quad |g_5\sigma_5| < 0.4 \ . \tag{19}$$

This fit indicates clearly that only the Γ_3 deformations play a role in determining the ESR line shape. To demonstrate this point we have plotted in the bottom of Fig. 2 a fit using the following three sets of parameters:

(a) $|g_3\sigma_3| = 1.6$, but $|\sigma_5 g_5| = 0$,
(b) $|g_3\sigma_3| = 0$, but $|g_5\sigma_5| = 1.32$,
(c) $|g_3\sigma_3| = 1.6$, and $|g_5\sigma_5| = 1.32$.

As clearly seen the effect of Γ_5 deformations would change the line shape substantially. Thus we conclude that the effect of Γ_5 deformations on the ESR spectra can be neglected.

IV. DISCUSSION

A. Correlation between magnetization and ESR: Determination of σ_3 for LaSb:Dy

Our ESR data yield information about $g_3\sigma_3$ to be $|g_3\sigma_3| = 1.6 \pm 0.03$. Note that this value is by a factor of 3 larger than that reported previously.[11] According to Eq. (11) g_3 is related to $V(\Gamma_3)$ with coefficients depending on the cubic crystal-field level scheme and wave functions. One can easily show that $g_3 \cong 52 V(\Gamma_3)$ for DySb and LaSb:Dy. This yields $|V(\Gamma_3)\sigma_3| = 0.03$ K. The magnetization as measured in the [001] direction yields a value for $V(\Gamma_3)$ to be $|V(\Gamma_3)| = 24$ K. Thus, a combination of the ESR data and the magnetization data gives $\sigma_3 = 1.25 \times 10^{-3}$. Note that the combination of these two experimental techniques yields information about σ_3 which could not be observed otherwise. The value of σ_3 for LaSb:Dy is of the same order of magnitude as the value of σ_3 observed by Oseroff and Calvo for Ag:Dy (Ref. 12) or Pela *et al.*[17] for Ag:Dy.

A question arises as to why the ESR data indicate that only Γ_3 strain modes are important, while the magnetization away from the [001] direction provides evidence that Γ_5 strains also play a role. The answer to this question is actually given by Eq. (11). Using this equation together with the appropriate energy splitting and wave function we have calculated

$$\frac{g_3}{g_5} \simeq 26 \frac{V(\Gamma_3)}{V(\Gamma_5)} \ . \tag{20}$$

Thus if $V(\Gamma_3)$ and $V(\Gamma_5)$ exhibit the same order of magnitude and so are σ_3 and σ_5, we expect the dominance of the Γ_3 strains in LaSb:Dy.

B. "Single ion" Jahn-Teller effects in LaSb:Dy and the origin of the random strains

In Fig. 5 we have plotted the free energy as a function of $\epsilon(\Gamma_{3g\theta})$ only (neglecting any contribution from $\Gamma_{3g\epsilon}$ and Γ_5 strain modes). The free energy was calculated using the parameters $x = -0.84$, $W = 0.4$ K, $C(\Gamma_3) = 420.000$ K/ion, $|V(\Gamma_3)| = 24$ K, $\vec{H}$ along the [100] direction, and equals $H = 1000$ G. The results are very interesting. At high temperatures the free energy exhibits a well-defined single minima at $\epsilon(\Gamma_{3g\theta}) = 0$. For temperatures lower than $T = 7$ K, a very flat minimum is observed. As the elastic constant of force is derived from the free energy by $C = \partial^2 F / \partial \epsilon^2$, it is clear that a softening of the elastic

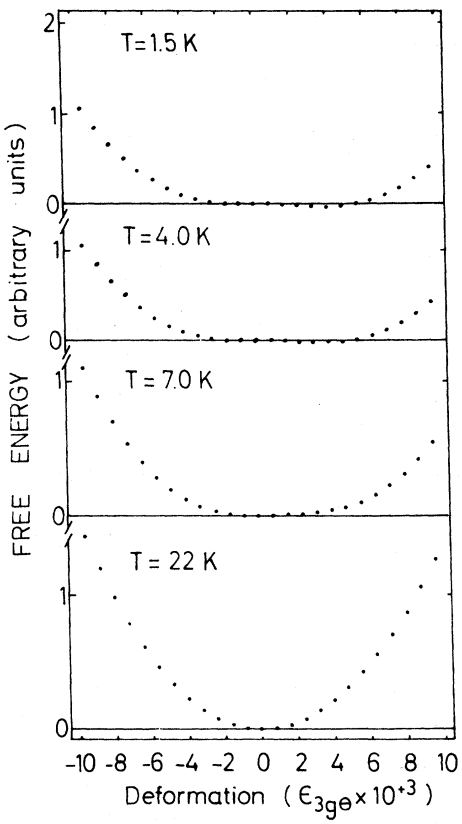

FIG. 5. Free energy, F, as a function of the $\epsilon(\Gamma_{eg\theta})$ strain for $\vec{H}$ along the [001] direction. The parameters used are $x = -0.84$, $W = 0.4$ K, $|V(\Gamma_3)| = 24$ K, $C(\Gamma_3) = 420.000$ K/ion, $H = 1$ kG.

constants of force occur at low temperatures.

We believe that this softening is partially responsible for the strains at low temperatures. The population of the free-energy surface is proportional to $\exp[-F(\epsilon)/k_BT]$ and consequently all the flat part of the free-energy surface in the vicinity of the minima has a finite probability to be populated. In short, the Dy ions are exposed to a large range of strains consistent with our ESR data.

The observation of strain effects at higher temperatures can be explained partially by Fig. 5. Although at high temperature the free energy exhibits a clear minimum at $\epsilon=0$ (see $T=22$ K in Fig. 5), at these temperatures the Dy ions are not confined to the bottom of $F(\epsilon)$ because a large k_BT yields an increase of $\exp[F(\epsilon)/k_BT]$ for $\epsilon\neq 0$. This means that even at high T the Dy ions are exposed to strains.

C. Comparison with Magnetostriction of LaSb:Dy

Recent magnetostriction study of LaSb:Dy (Ref. 18) was analyzed using a similar procedure to that described in the present paper: The free energy was calculated using the known parameters x, W, $C(\Gamma_3)$ for a given field $\vec{H}$ along the [100] direction and for a given temperature. $V(\Gamma_3)$ was treated as an unknown parameter. As occurs in Figs. 4 and 5 the free energy as a function of ϵ exhibits a minima. The position of these minima yields the most stable distortions, $\langle\epsilon\rangle$. The magnetostriction $\Delta L/L$ was assumed to be proportional to $\langle\epsilon\rangle$. These measurements yield $V(\Gamma_3)=20$ K for Dy:LaSb, slightly smaller than our value for $V(\Gamma_3)$. The difference is due, in our opinion, to the fact that magnetostriction gives the lattice distortion far away from the ion, it is, actually, the "long-range" tail of the distortion produced by the rare-earth ion in the lattice. Magnetization, however, reflects the lattice distortion in the immediate vicinity of the rare-earth ions. In the frame of our cluster model the magnetization yields a better value for $V(\Gamma_3)$.

V. CONCLUSIONS

(i) The free-energy calculation based on parameters extracted from our magnetization data provides strong evidence for "single-ion" Jahn-Teller effects at low temperatures for LaSb:Dy. The ESR data are consistent with this picture.

(ii) Combined ESR and magnetization yield information about $V(\Gamma_3)$ and the strain distribution σ_3 which could not be observed otherwise.

(iii) We have demonstrated that Γ_3 type of strains dominate in the case of ESR of LaSb:Dy.

Note added in proof. In our theoretical analysis, we have neglected the kinetic energy in the strain Hamiltonian. This kinetic energy of strain depends on the generalized momentum parameters (the canonical conjugates of the strain parameters). Now we are able to demonstrate that the kinetic energy terms canceled out in the expression for the magnetic moment in the classical limit. Thus our approach was correct. A complete theoretical treatment is planned to be given elsewhere.

ACKNOWLEDGMENTS

We wish to acknowledge with thanks the initial cooperation of and suggestions by C. Rettori and V. Zevin. One of us (J.M.B.) would like to thank R. Engelman for interesting discussions.

*Present address: Department of Electrical Engineering and Science, Moore School of Electrical Engineering, University of Pennsylvania, Philadelphia, Penn. 19104.

[1]G. A. Gehring and K. A. Gehring, Rep. Prog. Phys. 38, 1–89 (1975); C. Jaussand, P. Morin, and D. Schmitt, J. Magn. Magn. Mater. 22, 98 (1980), and references therein; R. Aleonard and P. Morin, Phys. Rev. B 19, 3868 (1979); P. Morin, D. Schmitt, and E. Du Tremolet de Lacheisserie, *ibid.* 21, 1742 (1980); D. K. Ray and J. Sivardiere, Solid State Commun. 19, 1053 (1976).

[2]P. M. Levy, P. Morin, and D. Schmitt, Phys. Rev. Lett. 42, 1417 (1979).

[3]J. M. Dixon, J. Phys. C 10, 833 (1977), in contrast to the interpretation of Dixon, Zevin, Shaltiel, and Zingg claim for the existence of static trigonal deformation in Pd:Er.

[4]E. Bucher, R. J. Birgeneau, J. P. Maita, G. P. Felcher, and T. O. Brun, Phys. Rev. Lett. 28, 246 (1972).

[5]M. E. Mullen, B. Luthi, P. S. Wang, E. Bucher, L. D. Longinotti, and J. P. Maita, Phys. Rev. B 10, 186 (1974).

[6]T. J. Moran, R. L. Thomas, P. M. Levy, and H. H. Chen, Phys. Rev. B 7, 3238 (1973).

[7]P. M. Levy, J. Phys. C 6, 3545 (1973).

[8]P. M. Levy and H. H. Chen, in *Magnetism and Magnetic Materials—1971,* edited by C. O. Graham and J. J. Rhyne, AIP Conf. Proc. No. 5 (AIP, New York, 1972), p. 373.

[9]K. R. Lea, M. J. M. Leask, and W. P. Wolf, J. Phys. Chem. Solids 23, 1381 (1974).

[10]J. S. Kouvel, T. O. Brun, and F. W. Korty, Physica (Utrecht) 86–88B, 1043 (1977); M. J. Sablik and Y. L. Wang, Phys. Rev. B 19, 2729 (1979), and references therein.

[11]D. Davidov, V. Zevin, J. M. Bloch, and C. Rettori, Solid State Commun. 17, 1279 (1975).

[12]S. B. Oseroff and R. Calvo, Phys. Rev. B 18, 3041 (1978).

[13]R. Orbach and H. J. Stapelton, in *Electron Paramagnetic Resonance,* edited by S. Geschwind (Plenum, New York, 1972).

[14]P. Fulde, in *Handbook on Physics and Chemistry of Rare-Earth,* edited by K. A. Gschneidner, Jr., and L. Eyring (North-Holland, Amsterdam, 1979); P. Thalmeier and P. Fulde, Z. Phys. B 22, 359 (1975).

[15]G. Feher and A. F. Kip, Phys. Rev. 98, 377 (1955).

[16]J. M. Bloch, Ph.D. thesis (unpublished).

[17]C. A. Pela, G. E. Barberis, J. F. Suassuna, and C. Rettori, Phys. Rev. B 21, 34 (1980).

[18]G. J. Niewenhuys, D. Davidov, H. U. Hafner, and J. M. Bloch, Solid State Commun. (in press).